Published in final edited form as:
Clin Cancer Res. 2011 June 1; 17(11): 3686–3696. doi:10.1158/1078-0432.CCR-10-3142.

A Novel Oncolytic Herpes Simplex Virus that Synergizes with Phosphatidylinositol 3-Kinase/Akt Pathway Inhibitors to Target Glioblastoma Stem Cells

Ryuichi Kanai, **Hiroaki Wakimoto**, **Robert L. Martuza**, and **Samuel D. Rabkin**
Brain Tumor Research Center, Department of Neurosurgery, Massachusetts General Hospital and Harvard Medical School, Boston, MA, 02114, USA.

Abstract

Purpose—To develop a new oncolytic herpes simplex virus (oHSV) for glioblastoma therapy that will be effective in glioblastoma stem cells (GSCs), an important and untargeted component of glioblastoma. One approach to enhance oHSV efficacy is by combination with other therapeutic modalities.

Experimental design—MG18L, containing a U_S3 deletion and an inactivating LacZ insertion in U_L39, was constructed for the treatment of brain tumors. Safety was evaluated after intracerebral injection in HSV-susceptible mice. The efficacy of MG18L in human GSCs and glioma cell lines *in vitro* was compared to other oHSVs, alone or in combination with PI3K/Akt inhibitors (LY294002, triciribine, GDC-0941, BEZ235). Cytotoxic interactions between MG18L and PI3K/Akt inhibitors were determined using Chou-Talalay analysis. *In vivo* efficacy studies were performed using a clinically relevant mouse model of GSC-derived glioblastoma.

Results—MG18L was severely neuroattenuated in mice, replicated well in GSCs, and had anti-glioblastoma activity *in vivo*. PI3K/Akt inhibitors displayed significant but variable anti-proliferative activities in GSCs, while their combination with MG18L synergized in killing GSCs and glioma lines, but not human astrocytes, through enhanced induction of apoptosis. Importantly, synergy was independent of inhibitor sensitivity. *In vivo*, the combination of MG18L and LY294002 significantly prolonged survival of mice, as compared to either agent alone, achieving 50% long-term survival in glioblastoma-bearing mice.

Conclusions—This study establishes a novel therapeutic strategy: oHSV manipulation of critical oncogenic pathways to sensitize cancer cells to molecularly-targeted drugs. MG18L is a promising agent for the treatment of glioblastoma, being especially effective when combined with PI3K/Akt pathway-targeted agents.

Keywords

Virotherapy; cancer stem cell; glioma

Introduction

Glioblastoma (GBM) is the most common and deadly primary brain tumor in adults (1). Despite advances in drug development, overall survival has not substantially improved. Recently, cancer stem or tumor-initiating cells have been isolated from solid tumors, including GBM, that are tumorigenic with characteristics of adult stem cells including; self-

Corresponding Author: Samuel D. Rabkin, Brain Tumor Research Center, MGH, 185 Cambridge St., CPZN-3800, Boston, MA 02114. rabkin@helix.mgh.harvard.edu.

renewal and differentiation into multiple lineages (2). Glioblastoma stem cells (GSCs) are thought to be important in GBM progression, heterogeneity, recurrence, and resistance to therapy, and provide an important target for the development of new therapies (3). Detailed molecular analysis of GBMs has shown that genetic alterations in the phosphatidylinositol 3-kinase (PI3K)/Akt pathway, including in PTEN and PIK3CA, occur in about 80% of tumors (4, 5). These molecular changes confer GBMs with proliferative and survival advantages and may play a role in regulating GSCs (6). There has been rapid growth in the development and clinical testing of small molecule inhibitors of the PI3K/Akt pathway, including for glioma (7). It has been reported that GSCs are sensitive to Akt inhibitors (8, 9). Unfortunately, the combination of genetic alterations and the number of cross-regulatory feedback loops in the PI3K/Akt pathway raise questions about the likely clinical efficacy of inhibitors alone (7, 10).

Oncolytic viruses are a distinct class of targeted anticancer agents with unique mechanisms of action compared to other cancer therapies; they selectively replicate in and kill cancer cells (oncolysis), amplifying themselves and spreading, but sparing normal tissue. The safety of oncolytic herpes simplex virus (oHSV) therapy has been demonstrated in clinical trials for glioblastoma; however efficacy remains anecdotal and needs improvement (11, 12). Combining oHSV with chemotherapeutic drugs is an effective strategy to improve overall efficacy and depending upon the specific oHSV mutations and drug, synergistic cancer cell killing can be observed (13). All oHSV vectors developed for clinical use in the brain contain deletions of the γ34.5 gene, the major viral neurovirulence factor, which is associated with attenuated replication, even in cancer cells, and an inability to replicate in GSCs (14, 15). To overcome these obstacles and target different tumorigenic pathways, we have developed a new class of oHSV vectors for the treatment of tumors in the brain that contain a deletion in the HSV-1 Us3 gene. Us3 encodes a serine-threonine kinase that among its many activities includes inhibition of virus-induced apoptosis and Akt activation (16-18). As apoptotic pathways are frequently dysfunctional in tumor cells, Us3 mutants should engender tumor selectivity based on enhanced apoptosis in normal cells, preventing further replication, as was found with R7041 ($Us3^{-}$) infected HUVEC (18). We previously reported that R7041: (1) was efficacious *in vitro* against a number of cancer cell lines, including glioma U87 and T98G, and *in vivo* against U87 subcutaneous tumors; (2) synergized with PI3K/Akt inhibitors; and (3) was safe after systemic delivery in the periphery (18). In order to extend these findings to human GSCs and intracerebral glioblastoma tumor models for possible clinical translation, we constructed a new multi-mutated oHSV, MG18L (Us3-deleted and UL39 (ICP6)-negative), which is safe after intracerebral inoculation, replicates well in GSCs, and synergizes with PI3K/Akt pathway inhibitors in killing GSCs *in vitro* and *in vivo* through enhanced apoptosis.

Materials and Methods

Cell lines and reagents

U87 and T98G human glioma and Vero (African green monkey kidney) cells were obtained from the American Type Culture Collection (ATCC, Manassas, VA) and used at low passage number. Human astrocytes were obtained from ScienCell (San Diego, CA). Cells were maintained in Dulbecco's modified Eagle's medium supplemented with 10% FCS (DMEM-FCS) at 37°C and 5% CO_2. Human GSCs were isolated as previously described and cultured in EF20 medium composed of Neurobasal medium (Invitrogen, Carlsbad, CA) supplemented with 3mM L-Glutamine (Mediatech, Manassas, VA), 1× B27 supplement (Invitrogen), 0.5× N2 supplement (Invitrogen), 2 μg/ml heparin (Sigma), 20 ng/ml human EGF (R&D systems, Minneapolis, MN), 20 ng/ml human FGF-2 (Peprotech, Rocky Hill, NJ) and 0.5× penicillin G/streptomycin sulfate/amphotericinB complex (Mediatech) (15). The stem-cell features of GBM4, GBM8 and BT74 have been previously described (15).

Spheres were dissociated using NeuroCult Chemical Dissociation kit (StemCell Technologies, Vancouver, BC, Canada). Passaged cells were confirmed to be mycoplasma-free. LY294002 (LC Laboratories, Woburn, MA), triciribine (Akt inhibitor V) (Santa Cruz Biotechnology, Santa Cruz, CA), GDC-0941 (Chemdea, Ridgewood, NJ), BEZ235 (Chemdea), and Z-VAD-FMK (Tocris bioscience, Ellisville, MI) were dissolved in dimethyl sulfoxide (Sigma-Aldrich, St. Louis, MO).

Viruses

All viruses were constructed on a HSV-1 strain F background. G207 (γ34.5Δ, ICP6^{-}, LacZ), G47Δ (γ34.5Δ, ICP6^{-}, ICP47/Us11proΔ, LacZ), and FΔ6 (ICP6^{-}, LacZ) have been previously described (14, 15, 19). R7041 (Us3-deleted) was provided by Dr. B. Roizman (University of Chicago) (20). Viruses were grown, purified, and titered on Vero cells (19).

Construction of MG18L

Construction and characterization of MG18L was as described (19). Briefly, the 5.3-kb fragment of pKX2-βG3 (from S.K. Weller, University of Connecticut Health Center), containing the E.coli *lacZ* sequence inserted in-frame in U_L39, was co-transfected with R7041 viral DNA into Vero cells using Lipofectamine (Invitrogen). Recombinant viruses, isolated by limiting dilution and identified as plaques staining blue after X-gal histochemistry (Fig S2A), were plaque purified three times in Vero cells. The genomic structure of MG18L was confirmed by restriction endonuclease digestion and Southern blot analysis (Fig S1).

Viral replication assay

Cell were seeded into 24-well plates (2×10^4 cells/well) in 0.5 ml of media and infected at a MOI of 1.5 in triplicate. LY294002 was added 6 hours post-infection and titers determined by plaque assay on Vero cells.

Cell susceptibility assays and Chou-Talalay analysis

Cells were seeded into 96-well plates (5000 cells/well), and 3.5 days after infection or 3 days after drug treatment MTS assays (Promega, Madison, WI) were performed according to manufacturer's instructions. For Chou-Talalay analysis (21), experiments were performed as described (22). Dose-response curves and 50% effective dose values (ED_{50}) were obtained, and fixed ratios of drug and virus and mutually exclusive equations used to determine combination indices (CIs). Briefly, combined dose-response curves were fitted to Chou-Talalay lines (21), which are derived from the law of mass action and described by the equation; log (*fa/fu*)=*m*log*D*-*m*log*Dm*, in which *fa* is the fraction affected, *fu* is the fraction unaffected, *D* is the dose, *Dm* is the median-effect dose, and *m* is the coefficient signifying the shape of the dose-response curve. The Combination Index values (CI) were calculated using the equation CI=(D1/D×1)+(D2/D×2)+(D1)(D2)/[(D×1)(D×2)], where D×1 and D×2 are the inhibitor and virus doses, respectively, that are required to achieve a particular *fa*, and D1 and D2 are the doses of the two agents (combined treatment) required for achieving the same *fa*. CI<1, =1, or >1 indicate synergistic, additive, and antagonistic interactions, respectively.

Immunoblots

Cells were treated with virus at MOI of 1.5, collected at indicated times after infection, and cell pellets lysed in RIPA buffer (Boston Bioproducts, Worcester, MA) with a cocktail of protease and phosphatase inhibitors (Roche, Indianapolis, IN). 12.5 μg of protein was separated by 10% SDS-PAGE and transferred to PVDF membranes by electroblotting. After blocking with 5% non-fat dry milk in TBS-Tween 20, membranes were incubated at 4°C

overnight with the following antibodies (1:1000) to: Akt, phosphorylated-Akt (Ser473), phosphorylated-Akt (Thr308), cleaved-PARP (all from Cell Signaling Technology, Danvers, MA), ICP4 (USBiological, Swampscott, MA), or Actin (Sigma), followed by incubation with appropriate HRP-conjugated goat anti-rabbit or anti-mouse secondary antibodies (1:5000, Promega) for 1 hour at room temperature. Protein-antibody complexes were visualized using ECL (Amersham Bioscience).

Assay of Caspase activity

Cells seeded into 96-well plates (5000 cells/well) in triplicate were infected, LY294002 (20 μM) or vehicle alone added 10 hours later, and caspase-3/-7 activity evaluated 16 hours after infection using the Caspase-Glo 3/7 Assay kit (Promega) according to the manufacturer's instruction.

Animal experiments

All *in vivo* procedures were approved by the Subcommittee on Research Animal Care at Massachusetts General Hospital. For safety evaluation, female A/J mice, 6 weeks of age (NCI, Frederick, MD), were stereotactically inoculated (right striatum, 2.5-mm lateral from Bregma and 2.5-mm deep) with virus in 3 μl of virus buffer (150mM NaCl, 20mM Tris, pH7.5) and euthanized when moribund. For efficacy studies, female athymic mice, 6-8 weeks of age (NCI) were stereotactically implanted (right striatum, 2.5-mm lateral from Bregma and 2.5-mm deep) with dissociated BT74 cells (1×10^5 in 3 μl). On day 8, randomly grouped mice were treated by intratumoral injection of MG18L or virus buffer in 3 μl, followed 12 hr later with intraperitoneal injection of LY294002 or solvent daily for 5 days. For mice surviving 100 days, the absence of tumor tissue was macroscopically confirmed. For histological studies, mice (28 days after tumor implantation) were treated with mock, MG18L and/or LY294002 (days 28 and 29). Upon sacrifice brains were removed, fixed in 4% paraformaldehyde, and frozen sections subjected to X-gal and hematoxylin staining or immunocytochemistry with antibodies against human specific nuclei (Millipore), cleaved caspase-3 (Cell Signaling Technology), nestin (Santa Cruz Biotech), or β-gal (mouse, Sigma or rabbit, Millipore), followed by incubation with appropriate FITC- and Cy3-conjugated secondary antibodies (Jackson ImmunoResearch, West Grove, PA) and DAPI.

Statistics

Comparisons of data in viral replication and caspase-3/7 assays were performed using a two-tailed Student *t*-test (unpaired). Survival was analysed by Kaplan-Meier curves with comparisons by Log-rank test. P values less than 0.05 were considered statistically significant.

Results

CNS safety and selectivity of MG18L

MG18L is a new oHSV generated for glioblastoma therapy that contains a deletion of the Us3 gene and a LacZ insertion inactivating ICP6 (UL39) (Fig 1A). As isogenic controls, we used FΔ6, containing only the same ICP6 insertion in strain F, and R7041 with only the Us3 deletion. Similar to G207, replication of MG18L was highly compromised in human astrocytes compared to parental R7041 and FΔ6. In U87 human glioma cells, MG18L replicated to a greater extent than G207 and somewhat less than R7041 and FΔ6 (Fig 1B). For oHSV to be translatable to the clinic for delivery in the brain, it is critical that it is not neuropathogenic. To examine this, highly HSV-1 susceptible A/J mice were inoculated intracerebrally and evaluated for neurologic symptoms. All mice inoculated with as little as 4×10^2 pfu of wild-type HSV1 (Strain F) died, whereas all mice inoculated with 4×10^6 pfu

of MG18L (the highest dose obtainable in 3 μl) or FΔ6 survived. In contrast, this dose of R7041 killed 90% of mice (Table 1). We further quantified neurologic deficits using a scoring scale for morbidity, with four of 6 mice inoculated with FΔ6 (4×10^6 pfu) showing moderate symptoms, while two of 8 mice inoculated with MG18L at this dose exhibited only mild transient symptoms (Fig 1C). At a 10-fold lower dose, only 2 of 6 R7041-inoculated mice did not show deficits (Fig 1C). Thus, we conclude that MG18L is safe and selective for glioma cells.

Effects of MG18L against human GSCs *in vitro*

All GSCs tested were susceptible to MG18L replication, with virus yield being similar to R7041 in GBM8 and GBM13 and 4-5 fold less in GBM4 and BT74, while G207 does not replicate (Fig 2A). One activity of Us3 protein is to inhibit Akt phosphorylation at Ser 473 induced by HSV infection (17, 18). Phosphorylation of Akt is induced by FΔ6 and G207 in GBM4 and BT74, even though G207 does not replicate, as illustrated by shut-off of immediate-early ICP4 expression (Fig 2B). In MG18L infected GSCs, p-Akt (S473 but not T308) levels are further increased and remain stable or continue to increase with time (Fig 2B). The *in vitro* efficacy of MG18L was compared to FΔ6 and G47Δ in GSCs. FΔ6 was most effective at killing GSCs, while MG18L was similar to G47Δ, except in GBM8 (Fig 3A). The virus yields for G47Δ and FΔ6 were previously reported (15). This was similar in glioma cell lines U87 and T98G (Fig S2B).

Human GSCs exhibit variable sensitivities to PI3K/Akt pathway inhibitors *in vitro*

The PI3K/Akt signaling pathway, commonly activated in cancer, is one of the most active targets for drug development. As a prelude to examining the interaction between MG18L and PI3K/Akt pathway inhibitors, we determined the GSC sensitivity to inhibitors of; PI3K (GDC-0941), Akt (triciribine), mTOR/PI3K (BEZ235) and nonspecific PI3K (LY294002) (23). GBM13 was the least sensitive to all 4 inhibitors, followed by BT74, while GBM4 and GBM8 were quite sensitive (Fig 3B). Triciribine (~250 μM) had no effect on GBM13 viability, so its ED_{50} was not obtainable. Both U87 and T98G exhibited a similar range of inhibitor sensitivities as BT74 (Table S1).

MG18L synergizes with PI3K/Akt pathway inhibitors to inhibit human GSCs *in vitro*

One of the rationales for the construction of MG18L was its postulated ability to sensitize cancer cells to PI3K/Akt pathway inhibitors. MG18L and LY294002 synergized in killing 3 of the 4 GSCs, while the interaction in human astrocytes was antagonistic to additive (Fig 3C-G). Synergy was dependent on the Us3 deletion, as the interactions of FΔ6 and G47Δ ($Us3^+$ oHSV) with LY294002 were mostly additive or antagonistic (Fig 3C-F). Similarly, the interactions in glioma cell lines (U87, T98G) were synergistic only for $Us3^-$ R7041 and MG18L (Fig S3A). Synergy in U87 cells was not affected by the order of addition (Fig S3A). As LY294004 has a broad inhibitor profile across many PI3Ks and protein kinases (24), we examined the interactions of MG18L with selective PI3K/Akt pathway inhibitors that have been in clinical trial. Both triciribine and GDC-0941 synergized with MG18L to kill GBM4 and BT74 (Fig 3H, I), while the dual PI3K/mTOR inhibitor BEZ235 only synergized in GBM13 (Fig 3J). Because GBM13 was resistant to triciribine (Fig 3B), we were unable to perform a synergy analysis, however, a non-toxic dose of triciribine (30 μM) enhanced killing by MG18L (data not shown). The interactions were similar in the glioma cells lines, with BEZ235 only strongly synergistic in T98G (Fig S3B-D).

The combination of MG18L and LY294002 activate apoptotic pathways in glioma cells *in vitro*

Treatment of BT74 or U87 cells with LY294002 did not increase MG18L replication and virus yield (Fig S4), indicating that this is not the mechanism underlying synergy. Because Us3 blocks apoptosis in HSV-infected cells (16, 25), we hypothesized that the combination of MG18L and PI3K/Akt pathway inhibitors enhanced apoptosis in glioma cells, contributing to the observed synergy. Caspase-3 and -7 are common effector caspases of both the intrinsic and extrinsic apoptotic pathways. GSCs and U87 infected with FΔ6 or MG18L showed increased levels of caspase-3/7 activity, with MG18L being significantly more effective than FΔ6 (Fig 4B, D, F, H, S5B). Treatment of all GSCs and U87 cells, except GBM8 where synergistic killing was not observed, with MG18L and LY294002 showed significantly higher activities of caspase-3/7, compared to treatment with either alone (Fig 4A-D, S5B). The combination of FΔ6 and LY294002 did not produce an increase in caspase activity (Fig 4A-D, S5B), further demonstrating the involvement of the lack of Us3. As an additional readout for apoptosis we examined cleaved poly (ADP-ribose) polymerase (PARP). Consistent with the results from the caspase-3/7 activity assay, an increased level of cleaved-PARP was observed with the combination, except for GBM8 (Fig. 4E-H, S5A). In all cells, including GBM8, LY294002 treatment inhibited Akt activation (Fig 4E-H, S5A). These results support the view that synergy is due to increased apoptosis. Blocking caspase activation with a pan-caspase inhibitor, Z-VAD-FMK, before treatment with MG18L and LY294002, impaired synergy in BT74, GBM4, and U87 cells (Fig 4I, S5C, D).

MG18L treatment of human GSC-derived intracerebral tumors

To evaluate the *in vivo* efficacy of MG18L, we used BT74-derived intracerebral tumors. Histopathologically, this GSC forms aggressive tumors with high levels of vascularity and intratumoral hemorrhage (Fig 5A upper) (15), a hallmark of GBM in humans. MG18L efficiently infected and spread within the tumor, as illustrated by the extensive X-gal staining at 36 hr post-infection, which was more extensive than at 12 hr (Fig 5A lower). Sections were doubly immunostained with antibodies against human nuclear antigen (identifies BT74 cells) and β-galactosidase (identifies MG18L-infected cells), confirming MG18L spread within the tumor tissue (Fig 5B). Most of the cells in the tumor stained positive for nestin and these were susceptible to MG18L infection (Fig S6). Treatment of mice bearing established BT74 tumors with a single injection of MG18L significantly extended their survival (Fig 5C). Median survival increased from 32.5 days for mock to 41 days with MG18L, with 1 animal surviving 100 days.

LY294002 enhances the therapeutic efficacy of MG18L *in vivo*

LY294002 treatment alone of BT74 tumor-bearing mice was only modestly effective, with a prolongation of median survival by 5.5 days (Fig 5C). Combination with MG18L was much more efficacious than either treatment alone, with 50% of mice surviving long-term (Fig 5C). At 100 days, when all surviving mice were sacrificed, we did not detect tumor macroscopically. Similar results were obtained in a U87 intracerebral tumor model (Fig S7). Because combination treatment increased apoptosis *in vitro* (Fig 4), we examined BT74 tumor sections from mice for the presence of apoptotic cells (cleaved caspase-3 immunocytochemistry). Mock-treatment did not induce detectable cleaved caspase-3 within the tumor, while LY294002 induced scattered positive cells (Fig 5D, E). In contrast, MG18L infection induced a significant number of cleaved caspase-3-positive cells, which was further increased in combination with LY294002 (Fig 5D-E), further supporting the hypothesis that apoptosis is a key mediator of improved efficacy.

Discussion

We have constructed a new oHSV vector, MG18L, containing a Us3 deletion and ICP6 mutation that is both 'safe' after intracerebral inoculation in HSV-susceptible mice and efficacious against GSCs, warranting clinical translation for glioblastoma and possibly other tumors. The non-essential HSV Us3 gene is a serine-threonine kinase with multiple biological functions, including blocking virus and exogenously induced apoptosis (16, 26), so that its loss should engender tumor selectivity, although this still remains to be demonstrated. In fact, Us3 mutants in both HSV-1 and HSV-2 have been shown to have oncolytic activity (18, 27). Other Us3 activities that may be pertinent include; phosphorylation of HDAC1 and 2 blocking activity (28), phosphorylation of interferon-gamma receptor α blocking downstream signaling (29), and inhibiting virus-induced Akt activation (17, 18). While R7041, with a single Us3 mutation, was found to be very attenuated for pathogenicity in the periphery (18, 30, 31), it was not after intracerebral inoculation (32, 33). We found that R7041 had an LD_{50} ~4×10^5 pfu in A/J mice, while others reported LD_{50}'s of 1.8×10^6 and 1×10^5 pfu (32, 34). Therefore, to improve safety, we combined the Us3 deletion with an ICP6 mutation that further attenuates neurovirulence (Fig 1C) and increases sensitivity to anti-virals, yet does not greatly reduce virus replication in GSCs (15, 35). After intracerebral inoculation, MG18L exhibited a favorable safety profile that was comparable to γ34.5 deletion mutants such as G207 and G47Δ, which have been safely administered to GBM patients (12, 14, 36).

MG18L replicates well in GSCs and glioma cell lines, but not human astrocytes, and was very cytotoxic to GSCs *in vitro*, similar to G47Δ but less than FΔ6. While the addition of the ICP6 mutation to Us3-deleted oHSV reduces replication in some GSCs, this is offset by decreased replication in astocytes and improved safety. The mechanism underlying MG18L selectivity for GSCs, as well as apoptotic pathway function, remains to be determined. As expected, GSC infection with MG18L induced higher levels of p-Akt than FΔ6 infection. There are at least 10 inhibitors targeting the PI3K/Akt pathway in clinical trial, including for glioma (7, 23). MG18L synergized with PI3K/Akt inhibitors (LY294002, triciribine, GDC-0941) in killing GSCs, except for GBM8, but not human astrocytes. Recently, it was reported that increased p-Akt, in response to DNA damaging agent doxorubicin, correlated with PI3K inhibitor synergy (37), possibly through a similar mechanism as with oHSV. Synergy was dependent on the Us3 deletion, as other oHSVs expressing Us3 (G47Δ and FΔ6) did not synergize (Fig 3). In contrast, synergy did not seem to correlate with how susceptible cells were to the PI3K/Akt inhibitors or MG18L alone, as the ED_{50}'s varied over 10-fold, and GBM8 had very similar sensitivities as GBM4 (Fig 3). Interestingly, the dual PI3K/mTOR inhibitor, BEZ235, was found to only synergize with MG18L in GBM13 and was mostly antagonistic in GBM4 and BT74. GBM13 was much less sensitive to the PI3K/Akt pathway inhibitors than the other GSCs and astrocytes, although synergy was also observed in T98G cells, which was quite sensitive to the inhibitors alone. GBM13 is the only GSC tested that did not express PTEN (data not shown), and T98G has a PTEN mutation (38). We tried to examine synergy with the mTOR inhibitor rapamycin, but could not obtain reliable dose response curves for analysis of synergy. However, when a single dose of rapamycin was combined with serial dilutions of MG18L in GBM4 or BT74, the reduction in cell viability was much less than additive, which may have contributed to the antagonistic interaction with BEZ235.

PI3K inhibition with LY294002 did not affect MG18L replication, which could have been one mechanism for synergy. Instead, the mechanism appears to be due to enhanced apoptosis in combination treated cells. Interestingly, only in MG18L-infected GBM8 cells was apoptosis not increased by LY294002. Thus, synergy with LY294002 could be impaired or abrogated in the presence of the pan-caspase inhibitor Z-VAD-FMK in BT74,

GBM4, and U87 cells (Fig 4, S5). This supports the view that apoptosis induced by HSV infection that is not blocked by Us3 is suppressed by activated Akt, balancing competing Us3 altered pathways, and making the cells very sensitive to inhibition of Akt signaling. Inhibition of the PI3K/Akt pathway in glioma has been reported to either induce apoptosis or autophagy (39-42), and sensitize cells to chemotherapy-induced apoptosis (43). LY294002 treatment of GSCs significantly induced apoptosis in GBM4 and GBM8, but not GBM13 or BT74. The range of interactions observed in the different GSCs illustrates the complexity of the PI3K/Akt pathway in glioblastoma, with its multiple feedback loops overlaid with genetic alterations at different nodes in the pathway, as well as potential interactions with the MEK pathway (44). Further genetic analysis of the GSCs may identify alterations underlying sensitivity to inhibitors at different steps in the PI3K/Akt pathway and provide insights for future stratification of patients in any clinical trials with inhibitors in this pathway.

As a proof of concept study, we examined the combination of LY294002 with MG18L for *in vivo* therapy in mice bearing BT74 tumors. Combination treatment significantly prolonged the survival of mice, with 50% long-term survivors, compared to either agent alone. Synergy *in vitro* resulted in a 6.5-fold reduction in LY294002 dose at the ED_{50}, to a more obtainable dose *in vivo*. While synergy *in vitro* was not affected by the temporal order of addition, for this *in vivo* experiment we administered MG18L prior to LY294002 to allow for induction of Akt activation by MG18L infection, followed by Akt inhibition by molecular targeting drugs. It will be important for clinical translation to further characterize the effect of administration schedule on efficacy with clinically relevant inhibitors. Although we found that the combination treatment increased apoptosis both *in vitro* (Fig 4) and *in vivo* (Fig 5D, E), there may be additional factors contributing to the enhanced efficacy of the combination *in vivo*. For example, the antiangiogenic properties of PI3K/Akt/mTOR inhibitors (45, 46), and disruption of tumor interstitial space produced by enhanced apoptosis may have helped the spread of MG18L in the tumor tissue (47). In summary, MG18L is effective in killing human glioma cells including GSCs, and the therapeutic efficacy can be enhanced by combination with PI3K/Akt pathway inhibitors. This strategy of using an oncolytic virus to alter a cancer pathway so that it sensitizes cancer cells to small molecule inhibitors that molecularly target these pathways is a novel one that should be applicable to other oHSV mutants, signaling pathways, and cancers.

Translational Relevance

Glioblastoma is an invariably lethal brain tumor. Glioblastoma stem cells (GSCs) are thought to be important in disease progression, recurrence, and resistance to therapy, providing an important target for the development of new therapies. Oncolytic herpes simplex viruses (oHSVs) hold promise for glioblastoma treatment; however, evidence for clinical efficacy remains elusive. One strategy to enhance the efficacy of Us3-deleted oHSV is combination with phosphatidylinositol 3-kinase (PI3K)/Akt pathway inhibitors. This study shows that oHSV-MG18L replicates well in GSCs, is efficacious in mice bearing GSC-derived brain tumors, yet non-neuropathogenic in mice. Notably, MG18L synergizes with PI3K/Akt inhibitors in killing GSCs and their intracerebral tumors. This study is the first to demonstrate effective targeting of cancer stem cells by the combination of oHSV and small molecule inhibitors. Synergy with MG18L may be utilized to increase efficacy of PI3K/Akt inhibitors. These data provide support for translation of this novel strategy in glioblastoma patients.

Supplementary Material

Refer to Web version on PubMed Central for supplementary material.

Acknowledgments

We thank Dr. Bernard Roizman (University of Chicago) for R7041, and Dr. Sandra K. Weller (University of Connecticut Health Center) for pKX2-βG3. We also thank Cecile Zaupa for assistance with virus constructions and Matthew Gardner for preliminary synergy experiments.

Grant Support: NIH Grant NS-032677 (RLM) and Department of Defense grant W81XWH-07-1-0359 (SDR)

References

1. Wen PY, Kesari S. Malignant gliomas in adults. N Engl J Med. 2008; 359:492–507. [PubMed: 18669428]
2. Visvader JE, Lindeman GJ. Cancer stem cells in solid tumours: accumulating evidence and unresolved questions. Nat Rev Cancer. 2008; 8:755–68. [PubMed: 18784658]
3. Cheng L, Bao S, Rich JN. Potential therapeutic implications of cancer stem cells in glioblastoma. Biochem Pharmacol. 2010; 80:654–65. [PubMed: 20457135]
4. CGAR Network. Comprehensive genomic characterization defines human glioblastoma genes and core pathways. Nature. 2008; 455:1061–8. [PubMed: 18772890]
5. Parsons DW, Jones S, Zhang X, Lin JC, Leary RJ, Angenendt P, et al. An integrated genomic analysis of human glioblastoma multiforme. Science. 2008; 321:1807–12. [PubMed: 18772396]
6. Bleau AM, Hambardzumyan D, Ozawa T, Fomchenko EI, Huse JT, Brennan CW, et al. PTEN/PI3K/Akt pathway regulates the side population phenotype and ABCG2 activity in glioma tumor stem-like cells. Cell Stem Cell. 2009; 4:226–35. [PubMed: 19265662]
7. Liu P, Cheng H, Roberts TM, Zhao JJ. Targeting the phosphoinositide 3-kinase pathway in cancer. Nat Rev Drug Discov. 2009; 8:627–44. [PubMed: 19644473]
8. Eyler CE, Foo WC, LaFiura KM, McLendon RE, Hjelmeland AB, Rich JN. Brain cancer stem cells display preferential sensitivity to Akt inhibition. Stem Cells. 2008; 26:3027–36. [PubMed: 18802038]
9. Gallia GL, Tyler BM, Hann CL, Siu IM, Giranda VL, Vescovi AL, et al. Inhibition of Akt inhibits growth of glioblastoma and glioblastoma stem-like cells. Mol Cancer Ther. 2009; 8:386–93. [PubMed: 19208828]
10. Engelman JA. Targeting PI3K signalling in cancer: opportunities, challenges and limitations. Nat Rev Cancer. 2009; 9:550–62. [PubMed: 19629070]
11. Aghi M, Rabkin S. Viral vectors as therapeutic agents for glioblastoma. Curr Opin Mol Ther. 2005; 7:419–30. [PubMed: 16248277]
12. Markert JM, Liechty PG, Wang W, Gaston S, Braz E, Karrasch M, et al. Phase Ib trial of mutant herpes simplex virus G207 inoculated pre-and post-tumor resection for recurrent GBM. Mol Ther. 2009; 17:199–207. [PubMed: 18957964]
13. Kanai R, Wakimoto H, Cheema T, Rabkin SD. Oncolytic herpes simplex virus vectors and chemotherapy: are combinatorial strategies more effective for cancer? Future Oncol. 2010; 6:619–34. [PubMed: 20373873]
14. Todo T, Martuza RL, Rabkin SD, Johnson PA. Oncolytic herpes simplex virus vector with enhanced MHC class I presentation and tumor cell killing. Proc Natl Acad Sci U S A. 2001; 98:6396–401. [PubMed: 11353831]
15. Wakimoto H, Kesari S, Farrell CJ, Curry WT Jr. Zaupa C, Aghi M, et al. Human glioblastoma-derived cancer stem cells: establishment of invasive glioma models and treatment with oncolytic herpes simplex virus vectors. Cancer Res. 2009; 69:3472–81. [PubMed: 19351838]
16. Leopardi R, Van Sant C, Roizman B. The herpes simplex virus 1 protein kinase US3 is required for protection from apoptosis induced by the virus. Proc Natl Acad Sci U S A. 1997; 94:7891–6. [PubMed: 9223283]
17. Benetti L, Roizman B. Protein kinase B/Akt is present in activated form throughout the entire replicative cycle of deltaU(S)3 mutant virus but only at early times after infection with wild-type herpes simplex virus 1. J Virol. 2006; 80:3341–8. [PubMed: 16537601]

18. Liu TC, Wakimoto H, Martuza RL, Rabkin SD. Herpes simplex virus Us3(−) mutant as oncolytic strategy and synergizes with phosphatidylinositol 3-kinase-Akt targeting molecular therapeutics. Clin Cancer Res. 2007; 13:5897–902. [PubMed: 17908985]
19. Mineta T, Rabkin SD, Yazaki T, Hunter WD, Martuza RL. Attenuated multi-mutated herpes simplex virus-1 for the treatment of malignant gliomas. Nature Medicine. 1995; 1:938–43.
20. Purves FC, Longnecker RM, Leader DP, Roizman B. Herpes simplex virus 1 protein kinase is encoded by open reading frame US3 which is not essential for virus growth in cell culture. J Virol. 1987; 61:2896–901. [PubMed: 3039176]
21. Chou TC, Talalay P. Quantitative analysis of dose-effect relationships: the combined effects of multiple drugs or enzyme inhibitors. Adv Enzyme Regul. 1984; 22:27–55. [PubMed: 6382953]
22. Aghi M, Rabkin S, Martuza RL. Effect of chemotherapy-induced DNA repair on oncolytic herpes simplex viral replication. J Natl Cancer Inst. 2006; 98:38–50. [PubMed: 16391370]
23. Courtney KD, Corcoran RB, Engelman JA. The PI3K pathway as drug target in human cancer. J Clin Oncol. 2010; 28:1075–83. [PubMed: 20085938]
24. Gharbi SI, Zvelebil MJ, Shuttleworth SJ, Hancox T, Saghir N, Timms JF, et al. Exploring the specificity of the PI3K family inhibitor LY294002. Biochem J. 2007; 404:15–21. [PubMed: 17302559]
25. Nishiyama Y, Murata T. Anti-apoptotic protein kinase of herpes simplex virus. Trends Microbiol. 2002; 10:105–7. [PubMed: 11864810]
26. Galvan V, Roizman B. Herpes simplex virus 1 induces and blocks apoptosis at multiple steps during infection and protects cells from exogenous inducers in a cell-type-dependent manner. Proc Natl Acad Sci U S A. 1998; 95:3931–6. [PubMed: 9520470]
27. Kasuya H, Nishiyama Y, Nomoto S, Goshima F, Takeda S, Watanabe I, et al. Suitability of a US3-inactivated HSV mutant (L1BR1) as an oncolytic virus for pancreatic cancer therapy. Cancer Gene Ther. 2007; 14:533–42. [PubMed: 17415379]
28. Poon AP, Gu H, Roizman B. ICP0 and the US3 protein kinase of herpes simplex virus 1 independently block histone deacetylation to enable gene expression. Proc Natl Acad Sci U S A. 2006; 103:9993–8. [PubMed: 16785443]
29. Liang L, Roizman B. Expression of gamma interferon-dependent genes is blocked independently by virion host shutoff RNase and by US3 protein kinase. J Virol. 2008; 82:4688–96. [PubMed: 18321964]
30. Kurachi R, Daikoku T, Tsurumi T, Maeno K, Nishiyama Y, Kurata T. The pathogenicity of a US3 protein kinase-deficient mutant of herpes simplex virus type 2 in mice. Arch Virol. 1993; 133:259–73. [PubMed: 8257288]
31. Sagou K, Imai T, Sagara H, Uema M, Kawaguchi Y. Regulation of the catalytic activity of herpes simplex virus 1 protein kinase Us3 by autophosphorylation and its role in pathogenesis. J Virol. 2009; 83:5773–83. [PubMed: 19297494]
32. Meignier B, Longnecker R, Mavromara-Nazos P, Sears AE, Roizman B. Virulence of and establishment of latency by genetically engineered deletion mutants of herpes simplex virus. Virology. 1988; 162:251–4. [PubMed: 2827384]
33. Nishiyama Y, Yamada Y, Kurachi R, Daikoku T. Construction of a US3 lacZ insertion mutant of herpes simplex virus type 2 and characterization of its phenotype in vitro and in vivo. Virology. 1992; 190:256–68. [PubMed: 1326804]
34. Esaki S, Goshima F, Katsumi S, Watanabe D, Ozaki N, Murakami S, et al. Apoptosis induction after herpes simplex virus infection differs according to cell type in vivo. Arch Virol. 2010; 155:1235–45. [PubMed: 20535504]
35. Varghese S, Rabkin SD. Oncolytic herpes simplex virus vectors for cancer virotherapy. Cancer Gene Ther. 2002; 9:967–78. [PubMed: 12522436]
36. Markert JM, Medlock MD, Rabkin SD, Gillespie GY, Todo T, Hunter WD, et al. Conditionally replicating herpes simplex virus mutant, G207 for the treatment of malignant glioma: results of a phase I trial. Gene Ther. 2000; 7:867–74. [PubMed: 10845725]
37. Wallin JJ, Guan J, Prior WW, Edgar KA, Kassees R, Sampath D, et al. Nuclear phospho-Akt increase predicts synergy of PI3K inhibition and doxorubicin in breast and ovarian cancer. Sci Transl Med. 2010; 2:48ra66.

38. Steck PA, Pershouse MA, Jasser SA, Yung WK, Lin H, Ligon AH, et al. Identification of a candidate tumour suppressor gene, MMAC1, at chromosome 10q23.3 that is mutated in multiple advanced cancers. Nat Genet. 1997; 15:356–62. [PubMed: 9090379]

39. Koul D, Shen R, Bergh S, Sheng X, Shishodia S, Lafortune TA, et al. Inhibition of Akt survival pathway by a small-molecule inhibitor in human glioblastoma. Mol Cancer Ther. 2006; 5:637–44. [PubMed: 16546978]

40. Takeuchi H, Kondo Y, Fujiwara K, Kanzawa T, Aoki H, Mills GB, et al. Synergistic augmentation of rapamycin-induced autophagy in malignant glioma cells by phosphatidylinositol 3-kinase/protein kinase B inhibitors. Cancer Res. 2005; 65:3336–46. [PubMed: 15833867]

41. Fujiwara K, Iwado E, Mills GB, Sawaya R, Kondo S, Kondo Y. Akt inhibitor shows anticancer and radiosensitizing effects in malignant glioma cells by inducing autophagy. Int J Oncol. 2007; 31:753–60. [PubMed: 17786305]

42. Koul D, Shen R, Kim YW, Kondo Y, Lu Y, Bankson J, et al. Cellular and in vivo activity of a novel PI3K inhibitor, PX-866, against human glioblastoma. Neuro Oncol. 2010; 12:559–69. [PubMed: 20156803]

43. Opel D, Westhoff MA, Bender A, Braun V, Debatin KM, Fulda S. Phosphatidylinositol 3-kinase inhibition broadly sensitizes glioblastoma cells to death receptor- and drug-induced apoptosis. Cancer Res. 2008; 68:6271–80. [PubMed: 18676851]

44. Efeyan A, Sabatini DM. mTOR and cancer: many loops in one pathway. Curr Opin Cell Biol. 2010; 22:169–76. [PubMed: 19945836]

45. Castellino RC, Durden DL. Mechanisms of disease: the PI3K-Akt-PTEN signaling node-- an intercept point for the control of angiogenesis in brain tumors. Nat Clin Pract Neurol. 2007; 3:682–93. [PubMed: 18046441]

46. Schnell CR, Stauffer F, Allegrini PR, O'Reilly T, McSheehy PM, Dartois C, et al. Effects of the dual phosphatidylinositol 3-kinase/mammalian target of rapamycin inhibitor NVP-BEZ235 on the tumor vasculature: implications for clinical imaging. Cancer Res. 2008; 68:6598–607. [PubMed: 18701483]

47. Nagano S, Perentes JY, Jain RK, Boucher Y. Cancer cell death enhances the penetration and efficacy of oncolytic herpes simplex virus in tumors. Cancer Res. 2008; 68:3795–802. [PubMed: 18483263]

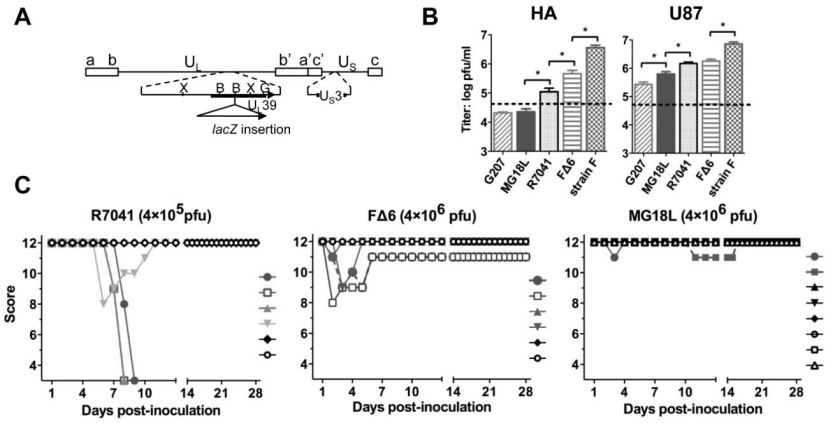

Figure 1. Characterization of MG18L

A. Schematic of MG18L, with *E. coli lacZ* coding sequence inserted into the U_L39 gene of R7041, which contains a deletion at Us3. Boxes represent inverted repeat sequences flanking the long (U_L) and short (U_S) unique sequences (B, *Bam*HI; G, *Bgl*II; X, *Xho*I). **B.** Replication of HSV-1 strain F and its derivatives in human astrocytes (HA) (left), and U87 (right). Cells were infected at MOI of 1.5, 24 hrs later cells and media were harvested and viral titers determined. Dotted lines indicate the input amount of virus. * $p<0.05$. **C.** Morbidity caused by intracerebral inoculation of HSV mutants evaluated with the following scoring scale; general appearance, spontaneous activity, reaction to external stimuli or neurological deficits, each scoring from 1-4 (with 1 severely impaired to 4 normal) for a total score of 3-12. Time course of morbidities caused by R7041 (4×10^5 pfu; left), FΔ6 (4×10^6 pfu; middle), and MG18L (4×10^6 pfu; right) indicated for each mouse (symbols).

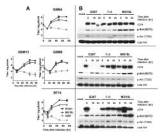

Figure 2. oHSV replication in GSCs and activation of Akt

GBM4 (upper), GBM8 (middle), GBM13 (middle), and BT74 (lower) were infected with G207, FΔ6, or MG18L at MOI of 1.5. **A.** Single step virus growth analysis. Cells and media were collected and virus yields determined. **B.** MG18L infection strongly activates Akt in GSCs. Collected cells were processed for western blotting with antibodies to ICP4 (immediate-early virus gene expression), phospho-Akt (Ser473 and Thr308), and total Akt.

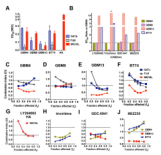

Figure 3. Effects of oHSV or PI3K/Akt pathway inhibitors on GSC viability and the interaction of the combination

A. GSCs and human astrocytes were infected with G47Δ, FΔ6, or MG18L at different MOIs and 3.5 days later viability was determined, dose-response curves obtained, and ED_{50} doses determined. **B.** Cell viability was determined 3 days after adding inhibitor. The ED_{50} dose for each GSC was normalized to the ED_{50} dose for GBM4 (13.2, 27.1, 0.57, and 0.034 μM for LY294002, triciribine, GDC-941, and BEZ235 respectively). **C-J.** Interactions were analyzed by the median effect method of Chou-Talalay, with data presented as Fraction affected–Combination Index plots. CI<1, =1, >1 represent synergistic, additive, and antagonistic interactions, respectively. (**C-G**) Interactions between oHSV (G47Δ, FΔ6 and MG18L) and LY294002 on proliferation of GBM4 (**C**), GBM8 (**D**), GBM13 (**E**), BT74 (**F**), and normal human astrocytes (**G**). (**H-J**) Interactions between MG18L and PI3K/Akt pathway inhibitors; triciribine (**H**), GDC-0941 (**I**) and BEZ235 (**J**).

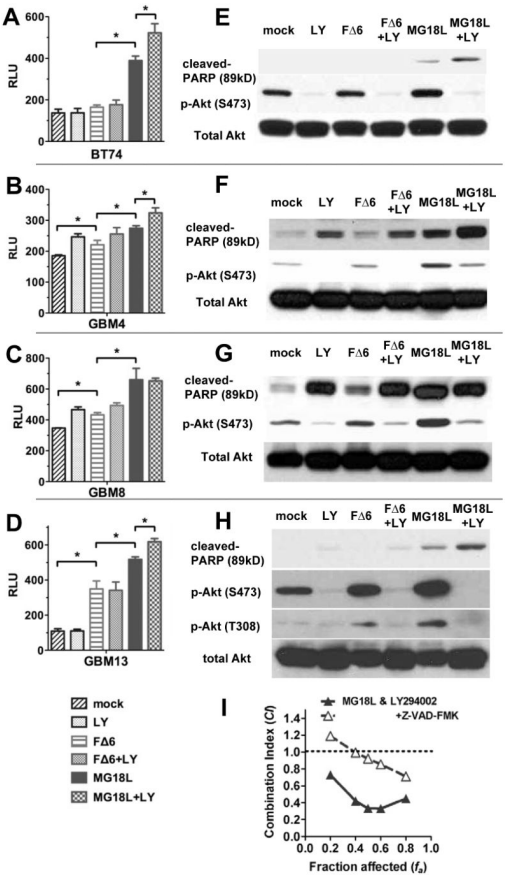

Figure 4. Combination of MG18L and LY294002 induces caspase-3/7 activation and PARP cleavage in GSCs

A-D. GSCs were infected with FΔ6 or MG18L at MOI of 1.5, or mock, and 14 hrs later cells were treated with or without LY294002 (LY; 20 μM), and the activities of caspase-3 and -7 were evaluated (RLU; relative luminescence units) 20 hrs after infection. **A**, BT74; **B**, GBM4; **C**, GBM8; **D**, GBM13. **E-H**. GSCs were treated as in A-D, except cells were collected and processed for western blotting with antibodies to cleaved PARP (apoptosis marker), phospho-Akt, and total Akt. **E**, BT74; **F**, GBM4; **G**, GBM8; **H**, GBM13. **I**. Synergy between MG18L and LY294002 in BT74 was impaired by the pan-caspase inhibitor Z-VAD-FMK (50 μM). The values for MG18L & LY204002 are the same as in Fig 3F.

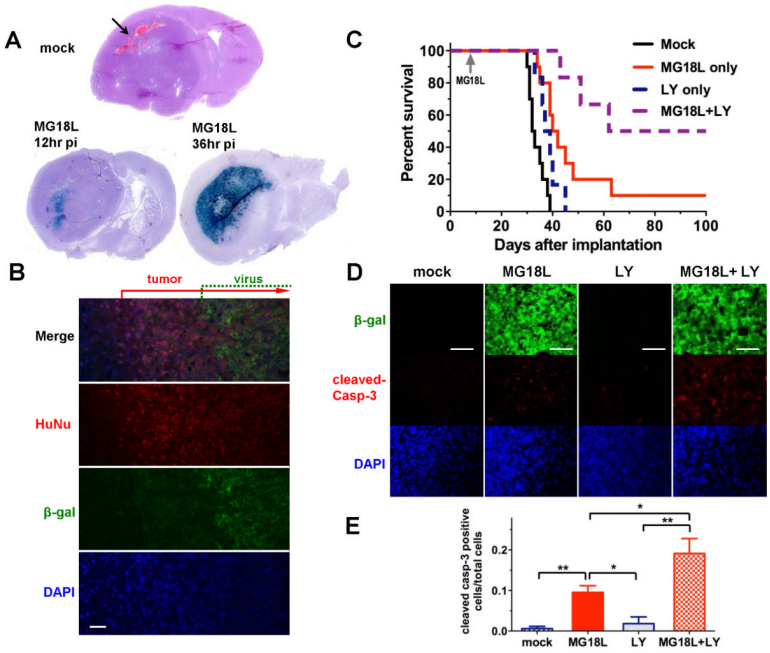

Figure 5. Combination therapy extends survival of mice bearing intracerebral BT74 tumors

A. (Upper) Athymic mice intracerebrally implanted with BT74 were sacrificed on day 30. Shown is a representative section of the brain with untreated BT74 tumor (H&E staining) illustrating intratumoral hemorrhage (arrow). (Lower) Mice treated with MG18L (2×10^6 pfu) on day 28 were sacrificed 12 hrs (left) and 36 hr (right) later. Sections were stained with X-gal (blue) to indicate MG18L infected cells. **B.** A region at the edge of the tumor from a 36 hr pi brain after immunostaining with antibodies against β-gal (green; MG18L infected cells) and human nucleus (red; BT74 cells), followed by DAPI (total nuclei) (scale bar = 100 μm). Virus was injected to the right of the displayed field. **C.** Kaplan-Meier survival curves of mice bearing BT74 tumors after treatment with intratumoral MG18L (2×10^6 pfu) or Mock, and intraperitoneal LY294002 (LY; 25mg/Kg/day) or vehicle (Mock, n=10; MG18L, n=10; LY294002, n=6; Combination n=6). $p<0.05$ (mock vs LY294002 and LY294002 vs MG18L+LY294002), <0.0005 (mock vs MG18L) (Log-rank test). **D.** Mice with BT74 tumors treated with mock, MG18L, LY294002, or the combination were sacrificed 36 hrs after MG18L injection. Brains were sectioned and tumors immunostained with antibodies to β-gal (green; MG18L) and cleaved caspase-3 (red; apoptosis) followed by DAPI (scale bars = 100μm). **E.** The ratio of cleaved caspase-3 positive cells/total was determined in three randomly selected fields (* $p < 0.05$, ** < 0.01).

Table 1

Safety evaluation of oHSV after intracerebral inoculation in A/J mice

Mice were observed for 28 days and the number of survivors / total indicated. NT, not tested

Dose [pfu]	Virus			
	Strain F (wild-type)	R7041	FΔ6	MG18L
4×10^6	NT	1/10	6/6	8/8
2.5×10^6	NT	NT	NT	3/3
4×10^5	NT	3/6	NT	NT
4×10^4	NT	6/6	NT	NT
4×10^3	0/3	NT	NT	NT
4×10^2	0/3	NT	NT	NT